Macroscopic capillarity without a constitutive capillary pressure function

R. Hilfer[a,b,*]

[a]*ICP, Universität Stuttgart, 70569 Stuttgart, Germany*
[b]*Institut für Physik, Universität Mainz, 55099 Mainz, Germany*

Abstract

This paper challenges the foundations of the macroscopic capillary pressure concept. The capillary pressure function, as it is traditionally assumed in the constitutive theory of two-phase immiscible displacement in porous media, relates the pressure difference between nonwetting and wetting fluid to the saturation of the wetting fluid. The traditional capillary pressure function neglects the fundamental difference between percolating and nonpercolating fluid regions as first emphasized in R. Hilfer [Macroscopic equations of motion for two phase flow in porous media, Phys. Rev. E 58 (1998) 2090]. The theoretical approach proposed here starts from residual saturations as the volume fractions of nonpercolating phases. The resulting equations of motion open the possibility to describe flow processes where drainage and imbibition occur simultaneously. The theory predicts hysteresis and process dependence of capillary phenomena. The traditional theory is recovered as a special case in the residual decoupling approximation. Explicit calculations are presented for quasistatic equilibrium profiles near hydrostatic equilibrium. The results are found to agree with experiment.
© 2006 Elsevier B.V. All rights reserved.

Keywords: Porous media; Multiphase flow; Immiscible displacement

1. Introduction and formulation of the problem

Already 65 years ago Leverett introduced the capillary pressure–saturation relation $P_c(S_W)$ into the macroscopic description of capillarity in porous media [1]. Despite its well-known limitations, this capillary pressure function has, in various disguises, remained the cornerstone of the theory of two phase flow in porous media until today [2–8].

My objective in this paper is to challenge the role of $P_c(S_W)$ as the central constitutive parameter. An alternative constitutive theory is presented in this paper. It is based, like the traditional theory, on volume fractions as primary unknowns, but does not introduce capillary pressure or relative permeabilities as constitutive parameters. Of course, the present theory of capillarity does contain the traditional theory as a special case, as will be seen below. Residual saturations of trapped fluids and their spatiotemporal changes are the basic new ingredient that distinguish the theory proposed here from existing ones. Existing theories, with the exception of [9–11], have neglected residual saturations as unknowns. My objective in this paper is to show

---

*Corresponding author. Institut für Computerphysik, Universität Stuttgart, Pfaffenwaldring 27, 70569 Stuttgart, Germany.

that a theory that includes residual saturations is both simpler and more comprehensive than the traditional theory.

Drainage and imbibition processes often occur simultaneously in realistic two phase flows, and they are accompanied by hysteresis effects. Explicit calculations for capillary hysteresis loops have remained a difficult problem, and there exists a large literature on the subject [9–26]. It is therefore appropriate to briefly review this literature.

Great attention was paid at first to the so-called Preisach model of independent domains [12–15] that was adapted to pore water hysteresis by Poulovassilis [16]. Later it was found that independent domain models cannot account in general for the hysteretic behaviour of pore water [17,18]. Other phenomenological approaches were based upon a similarity hypothesis [19–22]. Relative permeability hysteresis has been modeled along similar lines [23]. In such models boundary drainage or imbibition curves are rescaled. All these approaches are based on the traditional constitutive theory, and do not question the validity of the capillary pressure concept. Modern approaches, on the other hand, tend to modify the constitutive assumptions on a more basic level, and the present paper makes no exception.

A recent suggestion has been to modify the classical capillary pressure function with an additive term proportional to the rate of saturation change (see [24] and references therein). Another longstanding suggestion has been to introduce interfacial surface areas into the list of primary unknowns [9–11,25,26]. Other approaches have included even more variables such as interfacial velocities, entropies or mass densities [27]. However, these latter approaches suffer from a proliferation of unknowns and constitutive relations, and these constitutive relations are difficult to obtain. Finally, it should be mentioned that another approach to capillary hysteresis has been to abandon the macroscopic description in favour of microscopic (i.e., pore scale) network modeling [28,29].

An important motivation for searching alternative approaches are the unresolved problems with the traditional macroscopic theory that was introduced roughly 65 years ago [1,30,31], and has remained practically unchanged ever since. It is therefore adequate to remind the reader of some problems with the traditional theory. The biggest problem is the nonuniqueness of the capillary pressure function, and its inability to account for spatiotemporal changes of residual saturations. The traditional theory tacitly assumes that fluids trapped in pendular rings, ganglia or blobs behave in the same way as fluids that percolate to the sample surface. It implies that in hydrostatic equilibrium, when all velocities vanish, the pressures are everywhere hydrostatic, even in the trapped fluids. This is clearly not the case. Other problems, besides multivaluedness and hysteresis, arise from dynamic effects, and from the fact that there is frequently a confusion between pressures defined on the pore scale with macroscopically averaged pressure.

The approach followed in this paper was first introduced in Refs. [9–11,32]. It is based on the insight that the main effect of capillarity is the distinction between percolating and nonpercolating (trapped) fluid phases [9–11]. Percolation concepts are also crucial for the calculation of absolute permeabilities [33–40]. The fluids flow hydrodynamically in the percolating regions while the trapped fluids are kept in place by capillary forces. Trapped fluid can only move by viscous drag or through coalescence with percolating fluid regions.

Before defining the fundamental concepts of percolating and nonpercolating fluid phases in Section 3.1, it is appropriate to recall the constitutive assumptions of the traditional theory. This will be done in Section 2. The new theory is then presented in Section 3 following exactly the same outline as that of the traditional theory in Section 2. In this way the reader can clearly see the similarities and differences between the constitutive assumptions. Sections 4–6 are devoted to the analysis of the new equations. In Section 4 the special case of hydrostatic equilibrium is studied. Section 5 presents an approximation called residual decoupling approximation (RDA). It turns out that the traditional theory can be recovered from the new theory in the RDA. Finally, the last section presents solutions for quasistatic saturation profiles. It should be noted, and will be seen below, that the new theory, despite introducing two additional unknowns, requires fewer constitutive parameters than the traditional theory.

2. Theoretical formulation of the traditional theory

2.1. Phase structure

Consider the pore space (called $\mathbb{P}$) of a porous sample $\mathbb{S} = \mathbb{P} \cup \mathbb{M}$ with a rigid solid matrix (called $\mathbb{M}$). Within the traditional macroscopic theory one distinguishes two phases: a wetting phase, called water and

denoted as $\mathbb{W}$, plus a nonwetting phase, called oil and denoted as $\mathbb{O}$. From the macroscopic viewpoint the microscopic fluid configuration becomes smeared out. Hence the phases $\mathbb{W}$ and $\mathbb{O}$ are viewed as being simultaneously present at each macroscopic position $\mathbf{x}$.

2.2. Balance laws for mass, momentum and volume

The traditional theory starts from the fundamental balance laws of continuum mechanics for water $\mathbb{W}$ and oil $\mathbb{O}$. Recall the law of mass balance in differential form

$$\frac{\partial(\phi_i\varrho_i)}{\partial t} + \nabla \cdot (\phi_i\varrho_i\mathbf{v}_i) = M_i, \tag{1}$$

where $\varrho_i(\mathbf{x}, t), \phi_i(\mathbf{x}, t), \mathbf{v}_i(\mathbf{x}, t)$ denote mass density, volume fraction and velocity of phase $i = \mathbb{W}, \mathbb{O}$ as functions of position $\mathbf{x} \in \mathbb{S} \subset \mathbb{R}^3$ and time $t \in \mathbb{R}_+$. Exchange of mass between the two phases can be described through mass transfer rates M_i giving the amount of mass by which phase i changes per unit time and volume. Mass exchange terms are required when chemical reactions take place.

Momentum balance for the two fluids requires in addition

$$\phi_i\varrho_i \frac{\mathrm{D}^i}{\mathrm{D}t}\mathbf{v}_i - \phi_i\nabla \cdot \Sigma_i - \phi_i\mathbf{F}_i = \mathbf{m}_i - \mathbf{v}_iM_i, \tag{2}$$

where Σ_i is the stress tensor in the ith phase. $\mathbf{F}_i$ is the body force per unit volume acting on the ith phase, $\mathbf{m}_i$ is the momentum transfer into phase i from all the other phases, and $\mathrm{D}^i/\mathrm{D}t = \partial/\partial t + \mathbf{v}_i \cdot \nabla$ denotes the material derivative for phase $i = \mathbb{W}, \mathbb{O}$.

Defining the saturations $S_i(\mathbf{x}, t)$ as the volume fraction of pore space $\mathbb{P}$ filled with phase i one has the relation $\phi_i = \phi S_i$ where ϕ is the porosity of the sample. Expressing volume conservation $\phi_\mathbb{W} + \phi_\mathbb{O} = \phi$ in terms of saturations yields

$$S_\mathbb{W} + S_\mathbb{O} = 1. \tag{3}$$

In order to get the traditional theory these balance laws for mass, momentum and volume have to be combined with specific constitutive assumptions for M_i, $\mathbf{m}_i$, $\mathbf{F}_i$ and Σ_i.

2.3. General constitutive assumptions

As a first approximation it is usually assumed that the porous medium is macroscopically homogeneous

$$\phi(\mathbf{x}) = \phi = \text{const} \tag{4}$$

although this assumption can be relaxed, and rarely holds in practice [41]. Let us further assume that the fluids are incompressible so that

$$\varrho_\mathbb{W}(\mathbf{x}, t) = \varrho_\mathbb{W}, \tag{5a}$$

$$\varrho_\mathbb{O}(\mathbf{x}, t) = \varrho_\mathbb{O}, \tag{5b}$$

where the constants $\varrho_\mathbb{W}, \varrho_\mathbb{O}$ are independent of $\mathbf{x}$ and t. One assumes next that the stress tensor of the fluids is diagonal

$$\Sigma_\mathbb{W} = -P_\mathbb{W}\mathbf{1}, \tag{6a}$$

$$\Sigma_\mathbb{O} = -P_\mathbb{O}\mathbf{1}, \tag{6b}$$

where $P_\mathbb{W}, P_\mathbb{O}$ are the fluid pressures. Realistic subsurface flows have low Reynolds numbers so that the inertial term

$$\frac{\mathrm{D}^i}{\mathrm{D}t}\mathbf{v}_i = 0 \tag{7}$$

can be neglected in the momentum balance equation (18). It is further assumed that the body forces

$$\mathbf{F}_{\mathbb{W}} = \varrho_{\mathbb{W}}\mathbf{g}, \tag{8a}$$

$$\mathbf{F}_{\mathbb{O}} = \varrho_{\mathbb{O}}\mathbf{g} \tag{8b}$$

are given by gravity. As long as there are no chemical reactions between the fluids the mass transfer rates vanish, so that

$$M_{\mathbb{W}} = -M_{\mathbb{O}} = 0 \tag{9}$$

holds.

2.4. Viscous drag

Momentum transfer between the fluids and the rigid walls of the porous medium is assumed to be governed by viscous drag in the form

$$\mathbf{m}_{\mathbb{W}} = -\frac{\mu_{\mathbb{W}}\phi_{\mathbb{W}}^2}{k\,k_{\mathbb{W}}^r(S_{\mathbb{W}})}\mathbf{v}_{\mathbb{W}}, \tag{10a}$$

$$\mathbf{m}_{\mathbb{O}} = -\frac{\mu_{\mathbb{O}}\phi_{\mathbb{O}}^2}{k\,k_{\mathbb{O}}^r(S_{\mathbb{W}})}\mathbf{v}_{\mathbb{O}}, \tag{10b}$$

where $\mu_{\mathbb{W}}, \mu_{\mathbb{O}}$ are the constant fluid viscosities, k is the absolute permeability, and $k_{\mathbb{W}}^r(S_{\mathbb{W}}), k_{\mathbb{O}}^r(S_{\mathbb{W}})$ are the so-called relative permeabilities of water and oil.

2.5. Capillarity

Inserting the constitutive assumptions into the general balance laws (1)–(3) yields nine equations for 10 unknowns $S_{\mathbb{W}}, S_{\mathbb{O}}, P_{\mathbb{W}} P_{\mathbb{O}}, \mathbf{v}_{\mathbb{W}}, \mathbf{v}_{\mathbb{O}}$. An additional equation is needed. Based on observations of capillary rise in regular packings [42] it was argued in Ref. [1] that the pressure difference between oil and water should, in general, depend only upon saturation

$$P_{\mathbb{O}} - P_{\mathbb{W}} = \sigma_{\mathbb{W}\mathbb{O}}\kappa(S_{\mathbb{W}}) = P_c(S_{\mathbb{W}}), \tag{11}$$

where $\sigma_{\mathbb{W}\mathbb{O}}$ is the oil–water interfacial tension and $\kappa(S_{\mathbb{W}})$ is the mean curvature of the oil–water interface. This assumption has remained the cornerstone of the theory of macroscopic capillarity for 60 years, and it is being challenged here. The nonlinear constitutive parameter function $P_c(S_{\mathbb{W}})$ is called the capillary pressure–saturation relation and it is supposed to describe the macroscopic effect of capillarity in hydrostatic equilibrium (without flow). The functions $P_c(S_{\mathbb{W}})$ and $k_{\mathbb{W}}^r(S_{\mathbb{W}}), k_{\mathbb{O}}^r(S_{\mathbb{W}})$ are fit functions obtained from experiment. Popular fits have the general form [8, p. 56, 75]

$$P_c(S_{\mathbb{W}}) = P_c^{\dagger}\left(\frac{1 - S_e^{v_1}}{S_e^{v_2}}\right)^{v_3}, \quad P_c > 0, \tag{12a}$$

$$k_{\mathbb{W}}^r(S_{\mathbb{W}}) = k_{\mathbb{W}}^{r\,\dagger} S_e^{v_4}[1 - (1 - S_e^{v_5})^{v_6}]^{v_7}, \tag{12b}$$

$$k_{\mathbb{O}}^r(S_{\mathbb{W}}) = k_{\mathbb{O}}^{r\,\dagger}(1 - S_e^{v_8})^{v_9}(1 - S_e^{v_{10}})^{v_{11}}, \tag{12c}$$

where S_e is the effective saturation defined by

$$S_e = \frac{S_{\mathbb{W}} - S_{\mathbb{W}i}}{1 - S_{\mathbb{O}r} - S_{\mathbb{W}i}} \tag{13}$$

and $P_c^{\dagger}, k_{\mathbb{W}}^{r\,\dagger}, k_{\mathbb{O}}^{r\,\dagger}, S_{\mathbb{W}i}, S_{\mathbb{O}r}$ and $v_1, \ldots, v_{11}$ are 16 fit parameters. Note the restriction to $P_c > 0$. Frequently the number of parameters is reduced on the basis of calculations for capillary tube models. In the popular van-Genuchten model one assumes [8] $k_{\mathbb{W}}^{r\,\dagger} = k_{\mathbb{O}}^{r\,\dagger} = 1$, $v_1 = v_2 = v_5 = v_{10} = n/(n-1)$, $v_3 = 1/n$, $v_6 = 1 - (1/n)$, $v_7 = 2$, $v_8 = 1$ and $v_{11} = 2(n-1)/n$ where $n \in \mathbb{R}$.

3. Theoretical formulation of the new theory

3.1. Phase structure

The necessity to distinguish between percolating and nonpercolating fluid regions arises from the fact that in static equilibrium the pressure can become hydrostatic only in those fluid regions that are connected (or percolating) to the sample boundary [9–11]. Each of the two fluids $\mathbb{W}, \mathbb{O}$ consists of disjoint and pathconnected subsets (regions) $\mathbb{W}_i, \mathbb{O}_i$. More precisely, one has

$$\mathbb{W} = \bigcup_{i=1}^{N_{\mathbb{W}}} \mathbb{W}_i, \tag{14a}$$

$$\mathbb{O} = \bigcup_{i=1}^{N_{\mathbb{O}}} \mathbb{O}_i, \tag{14b}$$

where the subsets $\mathbb{W}_i, \mathbb{O}_i$ are mutually disjoint, and each of them is pathconnected. A set is called pathconnected if any two of its points can be connected by a path contained inside the set. The sets are called mutually disjoint if $\mathbb{O}_i \cap \mathbb{O}_j = \emptyset$ and $\mathbb{W}_i \cap \mathbb{W}_j = \emptyset$ holds for all $i \neq j$. The integers $N_{\mathbb{W}}, N_{\mathbb{O}}$ give the total number of pathconnected subsets for water (resp. oil). These numbers vary with time, as do the regions $\mathbb{W}_i, \mathbb{O}_i$.

Now define percolating ($\mathbb{F}_1, \mathbb{F}_3$) and nonpercolating ($\mathbb{F}_2, \mathbb{F}_4$) fluid regions by classifying the subsets $\mathbb{W}_i, \mathbb{O}_i$ as to whether they have empty or nonempty intersection with the sample boundary $\partial \mathbb{S}$. More formally, define

$$\mathbb{F}_1 = \bigcup_{\substack{i=1 \\ \partial \mathbb{W}_i \cap \partial \mathbb{S} \neq \emptyset}}^{N_{\mathbb{W}}} \mathbb{W}_i, \tag{15a}$$

$$\mathbb{F}_2 = \bigcup_{\substack{i=1 \\ \partial \mathbb{W}_i \cap \partial \mathbb{S} = \emptyset}}^{N_{\mathbb{W}}} \mathbb{W}_i, \tag{15b}$$

$$\mathbb{F}_3 = \bigcup_{\substack{i=1 \\ \partial \mathbb{O}_i \cap \partial \mathbb{S} \neq \emptyset}}^{N_{\mathbb{O}}} \mathbb{O}_i, \tag{15c}$$

$$\mathbb{F}_4 = \bigcup_{\substack{i=1 \\ \partial \mathbb{O}_i \cap \partial \mathbb{S} = \emptyset}}^{N_{\mathbb{O}}} \mathbb{O}_i, \tag{15d}$$

so that $\mathbb{F}_1$ is the union of all regions $\mathbb{W}_i$, and $\mathbb{F}_3$ is the union of all regions $\mathbb{O}_i$, that have nonempty intersection with the sample boundary $\partial \mathbb{S}$. Similarly $\mathbb{F}_2$ is the union of all regions $\mathbb{W}_i$ that have empty intersection with $\partial \mathbb{S}$, and similarly for $\mathbb{F}_4$. In this way each point in $\mathbb{P}$ belongs to one of four regions $\mathbb{F}_i$, $i = 1, 2, 3, 4$. This results in a total of four fluid phases called percolating (resp. nonpercolating) water, and percolating (resp. nonpercolating) oil. The index $i = 5$ will be used for the rigid matrix (=rock).

3.2. Balance laws for mass, momentum and volume

The approach presented here is based on the concept of volume fractions combined with the distinction between percolating and nonpercolating phases as introduced in Refs. [9–11] and discussed in Section 3.1. The volume fractions of the subsets $\mathbb{F}_i \subset \mathbb{S}, i = 1, 2, 3, 4$ and $\mathbb{M} \subset \mathbb{S}$ are denoted as $\phi_i(\mathbf{x}, t)$. Let ϕ denote the porosity (volume fraction of $\mathbb{P}$). Volume conservation implies the relations

$$\phi_1 + \phi_2 + \phi_3 + \phi_4 + \phi_5 = 1, \tag{16a}$$

$$S_1 + S_2 + S_3 + S_4 = 1, \tag{16b}$$

$$1 - \phi = \phi_5, \tag{16c}$$

where $\phi_i = \phi S_i$ $(i = 1, 2, 3, 4)$ are volume fractions, and S_i are saturations. The water saturation is defined as $S_{\mathbb{W}} = S_1 + S_2$, and the oil saturation as $S_{\mathbb{O}} = S_3 + S_4$.

The general law of mass balance in differential form reads $(i = 1, 2, 3, 4)$

$$\frac{\partial(\phi_i \varrho_i)}{\partial t} + \nabla \cdot (\phi_i \varrho_i \mathbf{v}_i) = M_i, \tag{17}$$

where $\varrho_i(\mathbf{x}, t), \phi_i(\mathbf{x}, t), \mathbf{v}_i(\mathbf{x}, t)$ denote mass density, volume fraction and velocity of phase $i = \mathbb{W}, \mathbb{O}$ as functions of position $\mathbf{x} \in \mathbb{S} \subset \mathbb{R}^3$ and time $t \in \mathbb{R}_+$. Exchange of mass between the two phases is described by mass transfer rates M_i giving the amount of mass by which phase i changes per unit time and volume. The law of momentum balance is formulated as $(i = 1, 2, 3, 4)$

$$\phi_i \varrho_i \frac{\mathrm{D}^i}{\mathrm{D}t} \mathbf{v}_i - \phi_i \nabla \cdot \Sigma_i - \phi_i \mathbf{F}_i = \mathbf{m}_i - \mathbf{v}_i M_i, \tag{18}$$

where Σ_i is the stress tensor in the ith phase, $\mathbf{F}_i$ is the body force per unit volume acting on the ith phase, $\mathbf{m}_i$ is the momentum transfer into phase i from all the other phases, and $\mathrm{D}^i/\mathrm{D}t = \partial/\partial t + \mathbf{v}_i \cdot \nabla$ denotes the material derivative for phase $i = \mathbb{W}, \mathbb{O}$.

3.3. General constitutive assumptions

For simplicity the porous medium is assumed to be macroscopically homogeneous. This assumption is formulated as

$$\phi(\mathbf{x}) = \phi = \mathrm{const} \tag{19}$$

although it is rarely valid in practice [41]. Realistic subsurface flows have low Reynolds numbers so that the inertial term

$$\frac{\mathrm{D}^i}{\mathrm{D}t} \mathbf{v}_i = 0 \tag{20}$$

can be neglected in the momentum balance equation (18). For incompressible fluids one has

$$\varrho_1(\mathbf{x}, t) = \varrho_{\mathbb{W}}, \tag{21a}$$

$$\varrho_2(\mathbf{x}, t) = \varrho_{\mathbb{W}}, \tag{21b}$$

$$\varrho_3(\mathbf{x}, t) = \varrho_{\mathbb{O}}, \tag{21c}$$

$$\varrho_4(\mathbf{x}, t) = \varrho_{\mathbb{O}}, \tag{21d}$$

independent of $\mathbf{x}, t$.

3.4. Viscous drag

The momentum transfer into phase i from all the other phases is assumed to be a simple viscous drag,

$$\mathbf{m}_i = \sum_{j=1}^{5} R_{ij}(\mathbf{v}_j - \mathbf{v}_i), \tag{22}$$

where the resistance coefficient R_{ij} quantifies the viscous coupling between phase i and j. For the rigid rock matrix $\mathbf{v}_5 = 0$. Hence $-R_{i5}\mathbf{v}_i$ is the momentum transfer from the wall into phase i. Then

$$\mathbf{m}_1 = R_{13}(\mathbf{v}_3 - \mathbf{v}_1) + R_{14}(\mathbf{v}_4 - \mathbf{v}_1) - R_{15}\mathbf{v}_1, \tag{23a}$$

$$\mathbf{m}_2 = R_{23}(\mathbf{v}_3 - \mathbf{v}_2) + R_{24}(\mathbf{v}_4 - \mathbf{v}_2) - R_{25}\mathbf{v}_2, \tag{23b}$$

$$\mathbf{m}_3 = R_{31}(\mathbf{v}_1 - \mathbf{v}_3) + R_{32}(\mathbf{v}_2 - \mathbf{v}_3) - R_{35}\mathbf{v}_3, \tag{23c}$$

$$\mathbf{m}_4 = R_{41}(\mathbf{v}_1 - \mathbf{v}_4) + R_{42}(\mathbf{v}_2 - \mathbf{v}_4) - R_{45}\mathbf{v}_4, \tag{23d}$$

where $R_{12} = 0$ and $R_{34} = 0$ was used because there is no common interface and hence no direct viscous interaction between these phase pairs. Each R_{ij} is a 3×3-matrix. In practice viscous coupling terms between the two fluid phases are often neglected.

3.5. Capillarity

The body forces are assumed to be given by gravity plus capillary forces

$$\mathbf{F}_1 = \varrho_1 \mathbf{g}, \tag{24a}$$

$$\mathbf{F}_2 = \varrho_2 \mathbf{g} + \mathbf{F}_{c\mathbb{W}}, \tag{24b}$$

$$\mathbf{F}_3 = \varrho_3 \mathbf{g}, \tag{24c}$$

$$\mathbf{F}_4 = \varrho_4 \mathbf{g} + \mathbf{F}_{c\mathbb{O}}, \tag{24d}$$

where the capillary body forces $\mathbf{F}_{c\mathbb{W}}, \mathbf{F}_{c\mathbb{O}}$ are responsible for keeping the trapped fluids inside the medium. They are assumed to be gradients of capillary potentials

$$\mathbf{F}_{c\mathbb{W}} = -\nabla \Pi_{c\mathbb{W}}, \tag{25a}$$

$$\mathbf{F}_{c\mathbb{O}} = -\nabla \Pi_{c\mathbb{O}}. \tag{25b}$$

The capillary potentials $\Pi_{c\mathbb{W}}, \Pi_{c\mathbb{O}}$ are defined as

$$\Pi_{c\mathbb{W}} = \Pi_{\mathrm{a}}^* - \Pi_{\mathrm{a}} S_1^{-\alpha}, \tag{26a}$$

$$\Pi_{c\mathbb{O}} = \Pi_{\mathrm{b}}^* - \Pi_{\mathrm{b}} S_3^{-\beta}, \tag{26b}$$

with constants $\Pi_{\mathrm{a}}^*, \Pi_{\mathrm{b}}^*, \Pi_{\mathrm{a}}, \Pi_{\mathrm{b}}$ and exponents $\alpha, \beta > 0$. For the purposes of the present paper $\Pi_{\mathrm{a}}^*, \Pi_{\mathrm{b}}^*$ can be set to zero without loss of generality.

The stress tensor for the percolating phases is specified in the same way as in the traditional theory through

$$\Sigma_1 = -P_1 \mathbf{1}, \tag{27a}$$

$$\Sigma_3 = -P_3 \mathbf{1}, \tag{27b}$$

where P_1 and P_3 are the fluid pressures. The stress tensor Σ_2, Σ_4 for the nonpercolating phases cannot be specified in the same way because the forces cannot propagate in nonpercolating phases. Here it is assumed that these stresses are given by the pressure in the surrounding percolating phase modified by the energy density stored in the common interface with the surrounding percolating phases. This suggests an Ansatz [32]

$$\Sigma_2 = (-P_3 + \gamma P_2^* S_2^{\gamma-1})\mathbf{1}, \tag{28a}$$

$$\Sigma_4 = (-P_1 + \delta P_4^* S_4^{\delta-1})\mathbf{1}, \tag{28b}$$

which can be motivated by geometrical considerations. Here, the constants P_2^*, P_4^* and exponents γ, δ are constitutive parameters, and Eq. (28) is taken as a constitutive assumption that has to be tested against experiment.

The mass transfer rates must depend on rates of saturation change. They are here tentatively assumed to be

$$M_1 = -M_2 = \eta_2 \phi \varrho_{\mathbb{W}} \left(\frac{S_2 - S_2^*}{S_{\mathbb{W}}^* - S_{\mathbb{W}}} \right) \frac{\partial S_{\mathbb{W}}}{\partial t}, \tag{29a}$$

$$M_3 = -M_4 = \eta_4 \phi \varrho_{\mathbb{O}} \left(\frac{S_4 - S_4^*}{S_{\mathbb{O}}^* - S_{\mathbb{O}}} \right) \frac{\partial S_{\mathbb{O}}}{\partial t}, \tag{29b}$$

where η_2, η_4 are constants. The parameters $S_{\mathbb{W}}^*, S_{\mathbb{O}}^*, S_2^*, S_4^*$ are defined by

$$S_{\mathbb{W}}^* = \frac{(1 - S_{\mathbb{O}\,\mathrm{im}})}{2}\left[1 - \tanh 1 \Big/ \left(\tau_{\mathbb{O}}\, \frac{\partial S_{\mathbb{O}}}{\partial t}\right)\right] + \frac{S_{\mathbb{W}\,\mathrm{dr}}}{2}\left[1 - \tanh 1 \Big/ \left(\tau_{\mathbb{W}}\, \frac{\partial S_{\mathbb{W}}}{\partial t}\right)\right], \tag{30a}$$

$$S_{\mathbb{O}}^* = 1 - S_{\mathbb{W}}^*, \tag{30b}$$

$$S_2^* = \frac{S_{\mathbb{W}\,\mathrm{dr}}}{2}\left[1 - \tanh 1 \Big/ \left(\tau_{\mathbb{W}}\, \frac{\partial S_{\mathbb{W}}}{\partial t}\right)\right], \tag{30c}$$

$$S_4^* = \frac{S_{\mathbb{O}\,\mathrm{im}}}{2}\left[1 - \tanh 1 \Big/ \left(\tau_{\mathbb{O}}\, \frac{\partial S_{\mathbb{O}}}{\partial t}\right)\right], \tag{30d}$$

where $S_{\mathbb{W}\,\mathrm{dr}}, S_{\mathbb{O}\,\mathrm{im}}$ are limiting saturations for S_2, S_4 and $\tau_{\mathbb{W}}, \tau_{\mathbb{O}}$ are time scales governing mass exchange.

4. Hydrostatic equilibrium

Consider first the case of hydrostatic equilibrium where $\mathbf{v}_i = 0$ for all i. In hydrostatic equilibrium all fluids are at rest. In this case the traditional theory ($i = \mathbb{W}, \mathbb{O}$) implies $\partial S_{\mathbb{W}}/\partial t = 0$ and $\partial S_{\mathbb{O}}/\partial t = 0$. The traditional momentum balance Eqs. (45) can be integrated to give

$$P_{\mathbb{W}}(\mathbf{x}) = P_{\mathbb{W}}(\mathbf{x}_0) + \varrho_{\mathbb{W}}\mathbf{g} \cdot (\mathbf{x} - \mathbf{x}_0), \tag{31a}$$

$$P_{\mathbb{O}}(\mathbf{x}) = P_{\mathbb{O}}(\mathbf{x}_0) + \varrho_{\mathbb{O}}\mathbf{g} \cdot (\mathbf{x} - \mathbf{x}_0), \tag{31b}$$

where $\mathbf{x}_0$ is an arbitrary fixed vector inside the sample. Combined with the assumption (11) one finds

$$P_{\mathrm{c}}(S_{\mathbb{W}}(\mathbf{x})) = P_{\mathbb{O}}(\mathbf{x}) - P_{\mathbb{W}}(\mathbf{x}) = P_{\mathrm{c}0} + (\varrho_{\mathbb{O}} - \varrho_{\mathbb{W}})\mathbf{g} \cdot (\mathbf{x} - \mathbf{x}_0) \tag{32}$$

implying the existence of a unique hydrostatic saturation profile $S_{\mathbb{W}}(\mathbf{x})$. Here $P_{\mathrm{c}0} = P_{\mathrm{c}}(\mathbf{x}_0)$ is the capillary pressure at $\mathbf{x} = \mathbf{x}_0$. Experiments show, however, that hydrostatic saturation profiles are not unique. As a consequence the traditional theory employs multiple $P_{\mathrm{c}}(S_{\mathbb{W}})$ relations for drainage and imbibition, and this leads to problems when imbibition and drainage occur simultaneously [43].

For the nonlinear theory proposed in this paper the equations of mass balance (17) imply $\partial S_i/\partial t = 0$ for all $i = 1, 2, 3, 4$. Integrating Eqs. (18) yields

$$P_1(\mathbf{x}) = P_1(\mathbf{x}_0) + \varrho_{\mathbb{W}}\mathbf{g} \cdot (\mathbf{x} - \mathbf{x}_0), \tag{33a}$$

$$P_3(\mathbf{x}) = P_3(\mathbf{x}_0) + \Pi_a(S_1(\mathbf{x})^{-\alpha} - S_1(\mathbf{x}_0)^{-\alpha}) + \gamma P_2^*(S_2(\mathbf{x})^{\gamma-1} - S_2(\mathbf{x}_0)^{\gamma-1}) + \varrho_{\mathbb{W}}\mathbf{g} \cdot (\mathbf{x} - \mathbf{x}_0), \tag{33b}$$

$$P_3(\mathbf{x}) = P_3(\mathbf{x}_0) + \varrho_{\mathbb{O}}\mathbf{g} \cdot (\mathbf{x} - \mathbf{x}_0), \tag{33c}$$

$$P_1(\mathbf{x}) = P_1(\mathbf{x}_0) + \Pi_b(S_3(\mathbf{x})^{-\beta} - S_3(\mathbf{x}_0)^{-\beta}) + \delta P_4^*(S_4(\mathbf{x})^{\delta-1} - S_4(\mathbf{x}_0)^{\delta-1}) + \varrho_{\mathbb{O}}\mathbf{g} \cdot (\mathbf{x} - \mathbf{x}_0). \tag{33d}$$

If one identifies P_1 with $P_{\mathbb{W}}$ and P_3 with $P_{\mathbb{O}}$ then Eqs. (33a,c) suggest to identify P_{c} as $P_3 - P_1$. Then Eqs. (33b) and (33d) combined with $S_1 = S_{\mathbb{W}} - S_2$ and $S_3 = 1 - S_{\mathbb{W}} - S_4$ imply $P_{\mathrm{c}} = P_{\mathrm{c}}(S_{\mathbb{W}}, S_2, S_4)$. Therefore, in the present theory, the pressure difference P_{c} in hydrostatic equilibrium depends not only on $S_{\mathbb{W}}$ but also on the residual saturations S_2 and S_4. This degeneracy of the hydrostatic limit seems to agree with experiment.

5. Residual decoupling approximation

Consider next the approach to hydrostatic equilibrium in the RDA [32]. Residual decoupling can be formulated mathematically as $\mathbf{v}_4 = \mathbf{0}, \mathbf{v}_2 = \mathbf{0}$ and $R_{23} = 0, R_{41} = 0$. Approach to hydrostatic equilibrium means that the velocities $\mathbf{v}_1, \mathbf{v}_3 \to 0$ are small but nonzero. In this case mass balance becomes

$$\frac{\partial S_1}{\partial t} + \nabla \cdot (S_1 \mathbf{v}_1) = \eta_2 \left(\frac{S_2 - S_2^*}{S_{\mathbb{W}}^* - S_{\mathbb{W}}}\right) \frac{\partial S_{\mathbb{W}}}{\partial t}, \tag{34a}$$

$$\frac{\partial S_2}{\partial t} = -\eta_2 \left(\frac{S_2 - S_2^*}{S_{\mathbb{W}}^* - S_{\mathbb{W}}}\right)\frac{\partial S_{\mathbb{W}}}{\partial t}, \tag{34b}$$

$$\frac{\partial S_3}{\partial t} + \nabla \cdot (S_3 \mathbf{v}_3) = \eta_4 \left(\frac{S_4 - S_4^*}{S_{\mathbb{O}}^* - S_{\mathbb{O}}}\right)\frac{\partial S_{\mathbb{O}}}{\partial t}, \tag{34c}$$

$$\frac{\partial S_4}{\partial t} = -\eta_4 \left(\frac{S_4 - S_4^*}{S_{\mathbb{O}}^* - S_{\mathbb{O}}}\right)\frac{\partial S_{\mathbb{O}}}{\partial t}. \tag{34d}$$

It is readily seen by insertion that Eqs. (34b) and (34d) admit the solutions

$$S_2(\mathbf{x}, t) = S_2^*(\mathbf{x}) + (S_{20}(\mathbf{x}) - S_2^*(\mathbf{x}))\left(\frac{S_{\mathbb{W}}^*(\mathbf{x}) - S_{\mathbb{W}}(\mathbf{x}, t)}{S_{\mathbb{W}}^*(\mathbf{x}) - S_{\mathbb{W}0}(\mathbf{x})}\right)^{\eta_2}, \tag{35a}$$

$$S_4(\mathbf{x}, t) = S_4^*(\mathbf{x}) + (S_{40}(\mathbf{x}) - S_4^*(\mathbf{x}))\left(\frac{S_{\mathbb{W}}(\mathbf{x}, t) - S_{\mathbb{W}}^*(\mathbf{x})}{S_{\mathbb{W}0}(\mathbf{x}) - S_{\mathbb{W}}^*(\mathbf{x})}\right)^{\eta_4}, \tag{35b}$$

where

$$S_{\mathbb{W}}(\mathbf{x}, t_0) = S_{\mathbb{W}0}(\mathbf{x}), \tag{36a}$$

$$S_2(\mathbf{x}, t_0) = S_{20}(\mathbf{x}), \tag{36b}$$

$$S_4(\mathbf{x}, t_0) = S_{40}(\mathbf{x}), \tag{36c}$$

are the initial conditions at some initial instant t_0. The limiting saturations $S_{\mathbb{W}}^*, S_{\mathbb{O}}^*, S_2^*, S_4^*$ are given by Eqs. (30). They depend only on the sign of $\partial S_{\mathbb{W}}/\partial t$. If $\partial S_{\mathbb{W}}/\partial t$ approaches zero from above then

$$S_{\mathbb{W}}^* = 1 - S_{\mathbb{O}\,\mathrm{im}}, \tag{37a}$$

$$S_{\mathbb{O}}^* = S_{\mathbb{O}\,\mathrm{im}}, \tag{37b}$$

$$S_2^* = 0, \tag{37c}$$

$$S_4^* = S_{\mathbb{O}\,\mathrm{im}} \tag{37d}$$

holds for imbibition processes (i.e., $\partial S_{\mathbb{W}}/\partial t > 0$). If $\partial S_{\mathbb{W}}/\partial t$ approaches zero from below then

$$S_{\mathbb{W}}^* = S_{\mathbb{W}\,\mathrm{dr}}, \tag{38a}$$

$$S_{\mathbb{O}}^* = 1 - S_{\mathbb{W}\,\mathrm{dr}}, \tag{38b}$$

$$S_2^* = S_{\mathbb{W}\,\mathrm{dr}}, \tag{38c}$$

$$S_4^* = 0 \tag{38d}$$

holds for drainage processes (i.e., $\partial S_{\mathbb{W}}/\partial t < 0$).

Note also that adding Eq. (34a) to Eq. (34b) resp. Eq. (34c) to Eq. (34d) reproduces the traditional law of mass balance

$$\frac{\partial S_{\mathbb{W}}}{\partial t} + \nabla \cdot (S_{\mathbb{W}} \mathbf{v}_{\mathbb{W}}) = 0, \tag{39a}$$

$$\frac{\partial S_{\mathbb{O}}}{\partial t} + \nabla \cdot (S_{\mathbb{O}} \mathbf{v}_{\mathbb{O}}) = 0, \tag{39b}$$

provided one identifies $\mathbf{v}_{\mathbb{W}}, \mathbf{v}_{\mathbb{O}}$ through the equations

$$S_{\mathbb{W}} \mathbf{v}_{\mathbb{W}} = S_1 \mathbf{v}_1 + S_2 \mathbf{v}_2, \tag{40a}$$

$$S_{\mathbb{O}}\mathbf{v}_{\mathbb{O}} = S_3\mathbf{v}_3 + S_4\mathbf{v}_4 \tag{40b}$$

as the barycentric velocities.

Momentum balance in the RDA becomes

$$\phi_1(\nabla P_1 - \varrho_{\mathbb{W}}\mathbf{g}) = R_{13}\mathbf{v}_3 - (R_1 + M_1)\mathbf{v}_1, \tag{41a}$$

$$0 = \phi_2(\nabla P_3 + \nabla \Pi_{c\mathbb{W}} - \gamma P_2^* \nabla S_2^{\gamma-1} - \varrho_{\mathbb{W}}\mathbf{g}), \tag{41b}$$

$$\phi_3(\nabla P_3 - \varrho_{\mathbb{O}}\mathbf{g}) = R_{31}\mathbf{v}_1 - (R_3 + M_3)\mathbf{v}_3, \tag{41c}$$

$$0 = \phi_4(\nabla P_1 + \nabla \Pi_{c\mathbb{O}} - \delta P_4^* \nabla S_4^{\delta-1} - \varrho_{\mathbb{O}}\mathbf{g}), \tag{41d}$$

where the abbreviations

$$R_1 = R_{13} + R_{14} + R_{15}, \tag{42a}$$

$$R_3 = R_{31} + R_{32} + R_{35}, \tag{42b}$$

were used. In accordance with the traditional theory [2] viscous coupling terms are neglected, i.e., $R_{31} = 0$ and $R_{13} = 0$. In addition it will be assumed here that $R_1 \gg M_1$, $R_3 \gg M_3$, and $S_i \neq 0$. With these assumptions one finds

$$\phi_1(\nabla P_1 - \varrho_{\mathbb{W}}\mathbf{g}) = -R_1\mathbf{v}_1 = -R_1\frac{\phi_{\mathbb{W}}}{\phi_1}\mathbf{v}_{\mathbb{W}}, \tag{43a}$$

$$\nabla P_3 = -\nabla \Pi_{c\mathbb{W}} + \gamma P_2^* \nabla S_2^{\gamma-1} + \varrho_{\mathbb{W}}\mathbf{g}, \tag{43b}$$

$$\phi_3(\nabla P_3 - \varrho_{\mathbb{O}}\mathbf{g}) = -R_3\mathbf{v}_3 = -R_3\frac{\phi_{\mathbb{O}}}{\phi_3}\mathbf{v}_{\mathbb{O}}, \tag{43c}$$

$$\nabla P_1 = -\nabla \Pi_{c\mathbb{O}} + \delta P_4^* \nabla S_4^{\delta-1} + \varrho_{\mathbb{O}}\mathbf{g}, \tag{43d}$$

where the barycentric velocities $\mathbf{v}_{\mathbb{W}}, \mathbf{v}_{\mathbb{O}}$ are defined through Eq. (40a). Subtracting Eq. (43a) from Eq. (43c), as well as Eq. (43d) from Eq. (43b), and equating the result gives

$$2(\varrho_{\mathbb{O}} - \varrho_{\mathbb{W}})\mathbf{g} + \frac{R_1}{\phi_1^2}\phi_{\mathbb{W}}\mathbf{v}_{\mathbb{W}} - \frac{R_3}{\phi_3^2}\phi_{\mathbb{O}}\mathbf{v}_{\mathbb{O}} = \nabla(\Pi_a S_1^{-\alpha} - \Pi_b S_3^{-\beta} + \gamma P_2^* S_2^{\gamma-1} - \delta P_4^* S_4^{\delta-1}), \tag{44}$$

where Eq. (26) has also been employed.

This result can be compared to the traditional theory. Inserting the constitutive assumptions (4)–(10) into Eqs. (2) gives the generalized Darcy laws

$$\phi_{\mathbb{W}}\mathbf{v}_{\mathbb{W}} = -\frac{k}{\mu_{\mathbb{W}}}k_{\mathbb{W}}^r(S_{\mathbb{W}})(\nabla P_{\mathbb{W}} - \varrho_{\mathbb{W}}\mathbf{g}), \tag{45a}$$

$$\phi_{\mathbb{O}}\mathbf{v}_{\mathbb{O}} = -\frac{k}{\mu_{\mathbb{O}}}k_{\mathbb{O}}^r(S_{\mathbb{W}})(\nabla P_{\mathbb{O}} - \varrho_{\mathbb{O}}\mathbf{g}) \tag{45b}$$

for the Darcy velocities $\phi_i\mathbf{v}_i$ [2, p. 155]. Combining this equation with (11) one finds

$$(\varrho_{\mathbb{O}} - \varrho_{\mathbb{W}})\mathbf{g} + \frac{\mu_{\mathbb{W}}}{kk_{\mathbb{W}}^r}\phi_{\mathbb{W}}\mathbf{v}_{\mathbb{W}} - \frac{\mu_{\mathbb{O}}}{kk_{\mathbb{O}}^r}\phi_{\mathbb{O}}\mathbf{v}_{\mathbb{O}} = \nabla P_c \tag{46}$$

in analogy with Eq. (44).

Comparison of Eq. (44) with (46) suggests to identify the capillary pressure up to a constant as

$$P_c(S_{\mathbb{W}}) = \tfrac{1}{2}[\Pi_a(S_{\mathbb{W}} - S_2)^{-\alpha} - \Pi_b(1 - S_{\mathbb{W}} - S_4)^{-\beta} + \gamma P_2^* S_2^{\gamma-1} - \delta P_4^* S_4^{\delta-1}], \tag{47}$$

where $S_2 = S_2(S_{\mathbb{W}})$ and $S_4 = S_4(S_{\mathbb{W}})$ are given by Eqs. (35). This result holds in the RDA combined with the assumptions above.

Furthermore, Eqs. (43a,c) become the generalized Darcy laws of the traditional theory, if the relative permeabilities are identified as

$$k_W^r(S_W) = 2R_1^{-1} \frac{\mu_W}{k} \phi^2 (S_W - S_2)^2, \tag{48a}$$

$$k_O^r(S_W) = 2R_3^{-1} \frac{\mu_O}{k} \phi^2 (1 - S_W - S_4)^2, \tag{48b}$$

where $S_2 = S_2(S_W)$ and $S_4 = S_4(S_W)$ are again given by Eqs. (35).

Figs. 1–3 illustrate these results. In Fig. 1 the pressure difference $P_3 - P_1$ is shown as a function of water saturation for various drainage and imbibition processes. The parameters were chosen in such a way that the primary drainage and imbibition curve reproduce measured experimental data. The experimental results are depicted as triangles (primary drainage) and squares (imbibition). The experiments were performed in a medium grained unconsolidated water wet sand of porosity $\phi = 0.34$. Water was used as wetting fluid while air (resp. TCE) were used as the nonwetting fluid. The experiments were carried out over a period of several weeks at the Versuchseinrichtung zur Grundwasser- und Altlastensanierung (VEGAS) at the Universität Stuttgart. They are described in more detail in Ref. [43]. The parameters for all the curves shown in all four figures are $S_{W\,dr} = 0.15$, $S_{O\,im} = 0.19$, $\alpha = 0.52$, $\beta = 0.90$, $\gamma = 1.5$, $\delta = 3.5$, $\eta_2 = 4$, $\eta_4 = 3$, $\Pi_a = 1620\,\text{Pa}$,
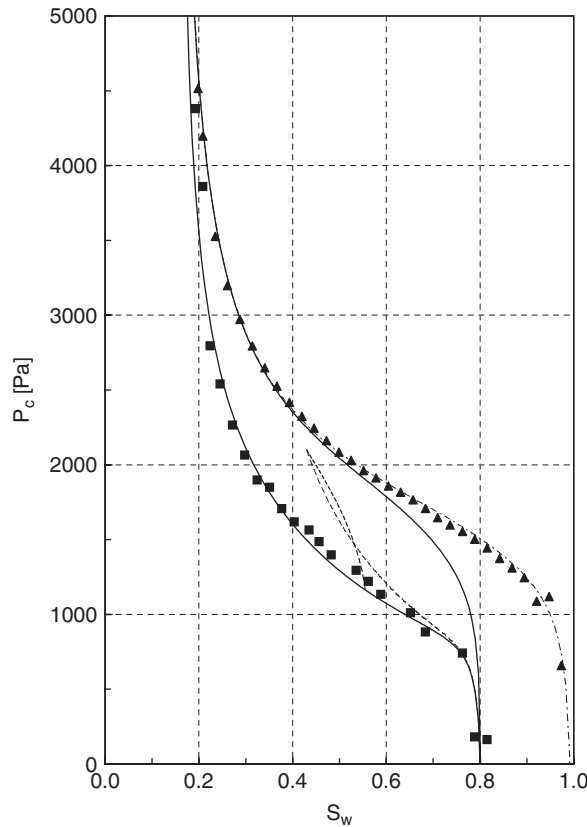
Fig. 1. Capillary pressure as function of water saturation S_W calculated from Eq. (47). Experimental data for primary drainage (triangles) and imbibition (squares) were obtained for a medium grained sand of porosity $\phi = 0.34$. The primary drainage curve is the dash-dotted line. The main hysteresis loop is the solid line. The two dashed lines are drainage and imbibition scanning curves. The drainage scanning curve starts from $S_W = 0.555$ on the boundary imbibition curve and goes to $S_W = 0.43$. The imbibition scanning curve starts from $S_W = 0.43$ on the drainage scanning curve and goes to the limiting $S_W = 1 - S_4^* = 0.81$ for imbibition processes. All curves in Figs. 1–4 have the same overall parameters: $S_{W\,dr} = 0.15$, $S_{O\,im} = 0.19$, $\alpha = 0.52$, $\beta = 0.90$, $\gamma = 1.5$, $\delta = 3.5$ $\eta_2 = 4$, $\eta_4 = 3$, $\Pi_a = 1620\,\text{Pa}$, $\Pi_b = 25\,\text{Pa}$, $P_2^* = 2500\,\text{Pa}$, $P_4^* = 400\,\text{Pa}$.
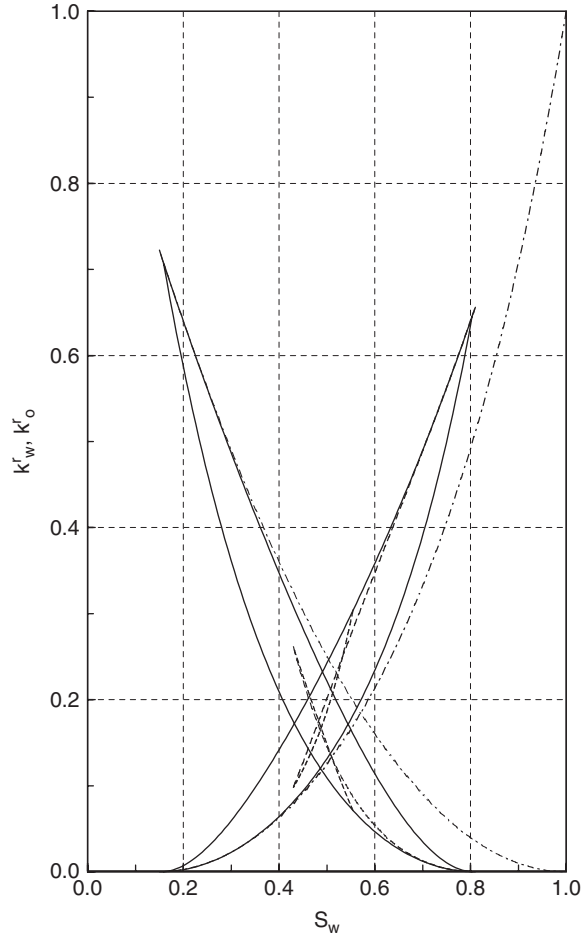
Fig. 2. Relative permeabilities $k_{\mathbb{W}}^r, k_{\mathbb{O}}^r$ calculated from Eq. (48) for the same displacement processes as shown in Fig. 1. Parameters and line styles are identical to those in Fig. 1.

$\Pi_b = 25\,\text{Pa}$, $P_2^* = 2500\,\text{Pa}$, and $P_4^* = 400\,\text{Pa}$. The temporal scales were taken as $\tau_{\mathbb{W}} = \tau_{\mathbb{O}} = 10^4\,\text{s}$ and $|\partial S_{\mathbb{W}}/\partial t| = 10^{-5}\,\text{s}^{-1}$.

6. Quasistatic saturation profiles close to the hydrostatic limit

To obtain more insight into the nature of the RDA it is necessary to integrate Eqs. (34) and (41). While this is analytically difficult for $\mathbf{v}_1 \neq 0$, $\mathbf{v}_3 \neq 0$, it is simple in the hydrostatic case when $\mathbf{v}_1 = 0$, $\mathbf{v}_3 = 0$. Therefore, it is now assumed that Eqs. (35) remain valid upon approach to the hydrostatic limit, i.e., for $\mathbf{v}_1, \mathbf{v}_3 \to 0$. Then Eqs. (41) can be integrated with respect to $\mathbf{x}$ in the same way as before, if one neglects all terms involving $\mathbf{v}_1, \mathbf{v}_3$. This leads to

$$P_1(\mathbf{x}, t) = C_1(t) + \varrho_{\mathbb{W}} \mathbf{g} \cdot \mathbf{x}, \tag{49a}$$

$$P_3(\mathbf{x}, t) + \Pi_a^* - \Pi_a S_1^{-\alpha} - \gamma P_2^* S_2^{\gamma-1} = C_2(t) + \varrho_{\mathbb{W}} \mathbf{g} \cdot \mathbf{x}, \tag{49b}$$

$$P_3(\mathbf{x}, t) = C_3(t) + \varrho_{\mathbb{O}} \mathbf{g} \cdot \mathbf{x}, \tag{49c}$$

$$P_1(\mathbf{x}, t) + \Pi_b^* - \Pi_b S_3^{-\beta} - \delta P_4^* S_4^{\delta-1} = C_4(t) + \varrho_{\mathbb{O}} \mathbf{g} \cdot \mathbf{x}, \tag{49d}$$
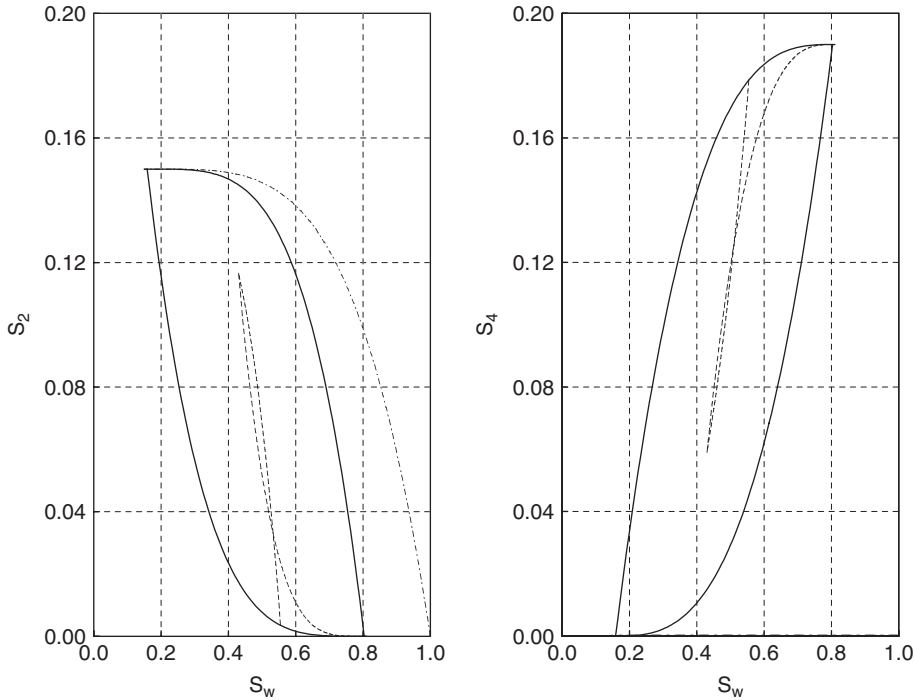
Fig. 3. Residual (nonpercolating) water saturation S_2 (left figure) and oil saturation S_4 (right figure) calculated from Eq. (35) as a function of total water saturation S_W. Parameters and line styles are identical to those in Figs. 1 and 2.

where $C_i(t)$ are integration constants. The first and third equations reflect the fact that the pressure in the percolating phases 1 and 3 is hydrostatic. Inserting (49c) into (49b) and (49a) into (49d) shows

$$C_3(t) - C_2(t) + \Pi_a^* + (\varrho_O - \varrho_W)\mathbf{g} \cdot \mathbf{x} = \Pi_a S_1^{-\alpha} + \gamma P_2^* S_2^{\gamma-1}, \tag{50a}$$

$$C_1(t) - C_4(t) + \Pi_b^* + (\varrho_W - \varrho_O)\mathbf{g} \cdot \mathbf{x} = \Pi_b S_3^{-\beta} + \delta P_4^* S_4^{\delta-1}. \tag{50b}$$

From $\partial S_i/\partial t = 0$ for $i = 1, 2, 3, 4$ follows that $C_i(t) = C_i = \text{const}$. Using volume conservation gives then

$$C_a + (\varrho_O - \varrho_W)\mathbf{g} \cdot \mathbf{x} = \Pi_a[S_W(\mathbf{x}) - S_2(\mathbf{x})]^{-\alpha} + \gamma P_2^* S_2(\mathbf{x})^{\gamma-1}, \tag{51a}$$

$$C_b + (\varrho_W - \varrho_O)\mathbf{g} \cdot \mathbf{x} = \Pi_b[1 - S_W(\mathbf{x}) - S_4(\mathbf{x})]^{-\beta} + \delta P_4^* S_4(\mathbf{x})^{\delta-1}, \tag{51b}$$

where $C_a = C_3 - C_2 + \Pi_a^*$ and $C_b = C_1 - C_4 + \Pi_b^*$. Inserting S_2, S_4 from Eqs. (35) yields two nonlinear equations that can be solved numerically for $S_W(\mathbf{x})$.

Further analysis of Eqs. (51) will from here on be restricted to the case of one dimension. Let this be the z-axis. The direction of gravity $\mathbf{g}$ is chosen to point along the negative z-direction, so that $\mathbf{g} \cdot \mathbf{x} = -gz$. If $\varrho_O < \varrho_W$ and $\Pi_a, \Pi_b, P_2^*, P_4^* > 0$ holds, then it is readily seen that the right-hand side remains nonnegative for all values of $z \in \mathbb{R}$ (note that also $S_2 \leqslant S_W$ and $\alpha, \beta, \gamma, \delta > 0$), while the left-hand side in Eq. (51a) becomes negative for $z \to -\infty$. It follows that Eq. (51a) cannot have physical solutions (obeying $0 \leqslant S_W \leqslant 1$) for $z \to -\infty$. Similarly, Eq. (51b) does not have physical solutions for $z \to \infty$. A unique physical solution for all z can be found by matching the solution $S_{Wa}(z)$ of Eq. (51a) for large z to the solution $S_{Wb}(z)$ of (51b) for small z at a unique intersection point $z = z^*$. This is achieved through fixing the difference $\Delta^* = |C_a - C_b|$ of the integration constants. The difference Δ^* is chosen in such a way that the solutions osculate at $z = z^*$. Any deviation from Δ^* will produce either two or zero intersection points between $S_{Wa}(z)$ and $S_{Wb}(z)$. The profiles

$S_{\mathbb{W}a}(z)$ and $S_{\mathbb{W}b}(z)$ are found by numerical solution of Eqs. (51) combined with Eqs. (35). For all subsequent calculations $C_1 = 0$, $C_4 = 0$, $\Pi_a^* = 0$ and $\Pi_b^* = 0$ has been assumed without loss of generality.

Fig. 4 shows the quasistatic saturation profiles for a process close to primary drainage. The initial saturations are assumed as $S_{20}(z) = 0$ and $S_{\mathbb{W}0}(z) = 1 - S_{40}(z) = 0.98$, i.e., the medium is almost fully saturated with water and contains initially a very small residual oil saturation of $S_{40}(z) = 0.02$. The time scales $\tau_{\mathbb{W}} = \tau_{\mathbb{O}} = 10^4$ s are unchanged, and the rate of saturation change is taken as $\partial S_{\mathbb{W}}(z, t)/\partial t = -10^{-5}$ s^{-1}. The integration constants are $C_a = 2250$ Pa and $C_b = 500$ Pa. Then the switch from $S_{\mathbb{W}a}(z)$ to $S_{\mathbb{W}b}(z)$ occurs at $z^* = 0.06$ m. Note that the drainage process creates irreducible (nonpercolating) water in the upper part of the sample. The profile $S_2(z)$ describing this nonpercolating water is seen as the leftmost of the three solid lines in Fig. 4. The water profile $S_{\mathbb{W}}(z)$ is seen as the central S-shaped solid line. Its shape is familiar from the traditional theory. Finally, the small residual (nonpercolating) oil profile $S_4(z)$ is seen as the rightmost solid line. It diminishes to zero in the upper part of the sample.

Next, consider an imbibition process starting from the same primary drainage profiles that are shown in Fig. 4. The flow process corresponds to a rising water table, e.g. through injecting water from below or withdrawing oil from the top. The three dotted curves in Fig. 5 are the initial profiles, and they are identical to the three solid lines in Fig. 4. The quasistatic profiles resulting from the imbibition are shown as the three solid lines in Fig. 5. Now, the rate of saturation change was $\partial S_{\mathbb{W}}/\partial t = 10^{-5}$ s^{-1}. The integration constants reflecting the pressure changes are $C_a = 500$ Pa, $C_b = 1835$ Pa. The switch between solutions occurs at $z^* = 0.619$ m.
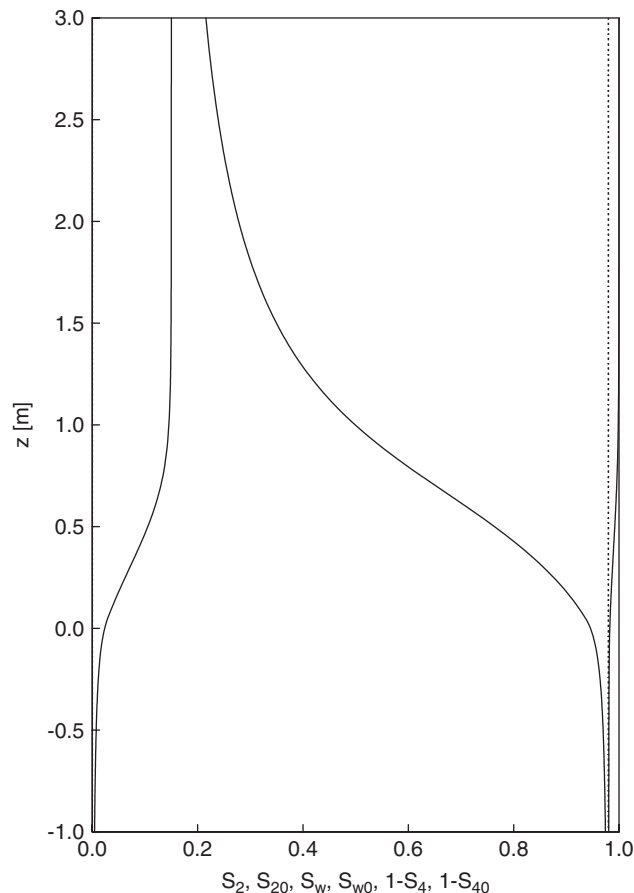
Fig. 4. Quasistatic primary drainage profiles (solid lines) as function of height z for $S_2(z)$ (left solid line), $S_{\mathbb{W}}(z)$ (center solid line), and $1 - S_4(z)$ (right solid line). The initial profiles (dotted lines) were spatially constant $S_{20}(z) = 0$ (left), $S_{\mathbb{W}0}(z) = 1 - S_{40}(z) = 0.98$ (right). The rate of saturation change is $\partial S_{\mathbb{W}}(z, t)/\partial t = -10^{-5}$ s^{-1}. The integration constants are $C_a = 2250$ Pa, $C_b = 500$ Pa, and the switch occurs at $z^* = 0.06$ m.
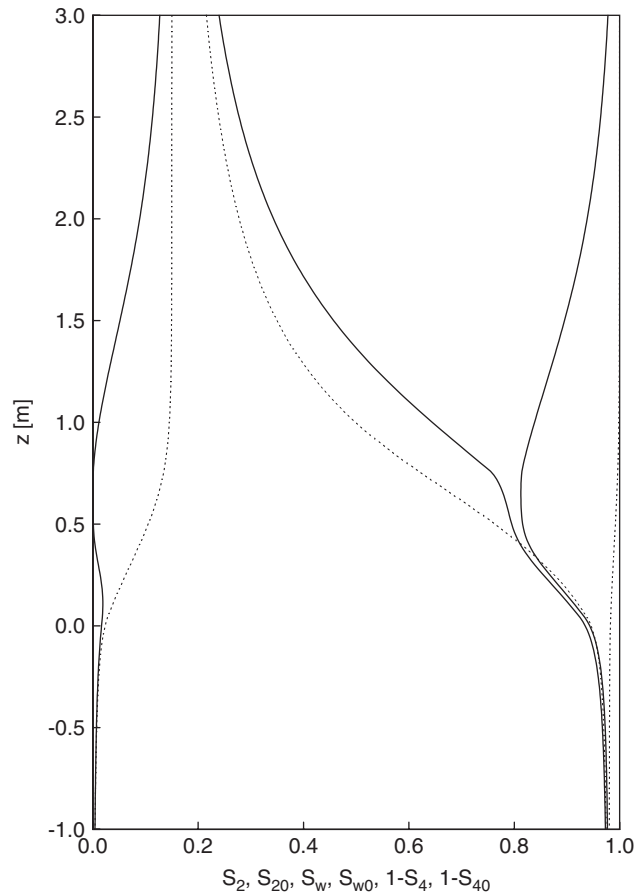
Fig. 5. Quasistatic saturation profiles $S_2(z)$ (left solid line), $S_W(z)$ (center solid line) and $1 - S_4(z)$ (right solid line) as a function of height z starting from the drainage profile shown in Fig. 4. The initial drainage profiles $S_{20}(z)$, $S_{W0}(z)$ and $S_{40}(z)$ (from left to right) are shown as dotted lines. The rate of saturation change was $\partial S_W/\partial t = 10^{-5}\,\mathrm{s}^{-1}$. The integration constants are $C_a = 500\,\mathrm{Pa}$, $C_b = 1835\,\mathrm{Pa}$, and $z^* = 0.619\,\mathrm{m}$.

Some of the profiles are nonmonotonic. The nonpercolating water phase was strongly reduced by the rising water table, and a "hole" appears between $z = 0.5$ and $1\,\mathrm{m}$. Correspondingly the nonpercolating oil phase has acquired a maximum around $z = 0.5\,\mathrm{m}$. The total water profile shows that the imbibition process takes place only in the upper part of the profile. The lower part of the sample has remained unaffected. This example demonstrates a difference to the traditional theory. The quasistatic profile for a drainage followed by imbibition can coexist with a unique S-shaped $P_c(S_W)$ relation. The strict relationship between static profiles and the $P_c(S_W)$ relation seems not to carry over into the RDA.

Finally, consider a soil column that is initially filled with a constant total water saturation of $S_{W0}(z) = 0.5$. Such an initial saturation could be achieved by rapidly turning a horizontal soil column into a vertical position. Assume that the initial nonpercolating saturations are $S_{20}(z) = 0.03$ and $S_{40}(z) = 0.05$. In this case the upper part of the column will be drained while the lower will show imbibition. The resulting quasistatic saturation profiles calculated within the RDA are displayed in Fig. 6. The process changes from drainage for $z > 0.59\,\mathrm{m}$ to imbibition for $z < 0.59\,\mathrm{m}$. In the example the integration constants are $C_a = 1900\,\mathrm{Pa}$ and $C_b = 323\,\mathrm{Pa}$. The switch between Eq. (51a) and Eq. (51b) occurs at $z^* = 0.06\,\mathrm{m}$. It is interesting to note that a kink appears at the initial saturation value. This could result from the assumption that $\partial S_W/\partial t$ switches abruptly at $z = 0.59$ from -10^{-5} to $10^{-5}\,\mathrm{s}^{-1}$. In a dynamic calculation the switching does not take place abruptly, and the kink might become smeared out.
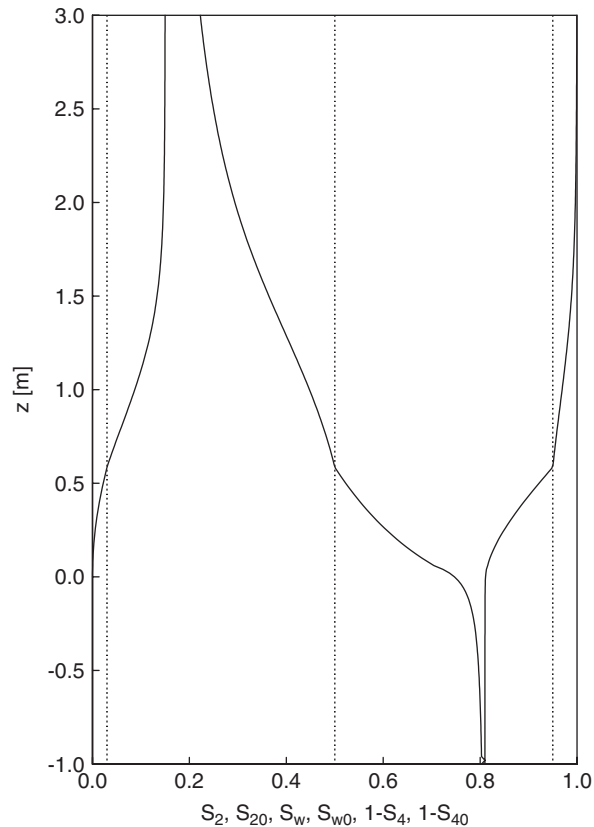
Fig. 6. Quasistatic saturation profiles $S_2(z)$ (left solid line), $S_W(z)$ (center solid line) and $1 - S_4(z)$ (right solid line) as a function of height z starting from initially constant profiles $S_{20}(z) = 0.03$ (left dotted line), $S_{W0}(z) = 0.5$ (center dotted line), and $S_{40}(z) = 0.05$ (right dotted line). The process changes from drainage to imbibition at $z = 0.59$ m. The rate of saturation change was $\partial S_W/\partial t = -10^{-5}\,\mathrm{s}^{-1}$ for $z > 0.59$ m corresponding to a drainage process, and $\partial S_W/\partial t = 10^{-5}\,\mathrm{s}^{-1}$ for $z < 0.59$ corresponding to an imbibition process. The integration constants are $C_a = 1900$ Pa, $C_b = 323$ Pa. The upper to lower profile switch happens at $z^* = 0.06$ m.

7. Conclusion

A generalization of the traditional theory of macroscopic capillarity in porous media was presented in this paper. It reproduces all experimental observations on hysteresis and process dependence of capillary pressure and relative permeabilities. The approach is based on the distinction between percolating and nonpercolating fluid phases introduced in Refs. [9–11]. The balance laws for mass, volume and momentum were augmented with a complete set of constitutive assumptions. The resulting equations were analyzed in the special limiting cases of hydrostatic equilibrium, and for the case of the RDA. Quastistatic saturation profiles were calculated numerically, and a capillary pressure–saturation relation was found analytically. The paper suggests that the time honoured concept of a capillary pressure function should be critically reviewed, and that the residual saturations are to a large extent responsible for the hysteresis and process dependence observed in experiment.

Acknowledgments

References

[1] M. Leverett, Capillary behaviour in porous solids, Trans. AIME 142 (1941) 152.

[2] A. Scheidegger, The Physics of Flow through Porous Media, University of Toronto Press, Canada, 1957.

[3] R. Collins, Flow of Fluids through Porous Materials, Reinhold Publishing Co., New York, 1961.

[4] R. de Wiest, Flow through Porous Media, Academic Press, New York, 1969.

[5] J. Bear, Dynamics of Fluids in Porous Media, Elsevier, New York, 1972.

[6] G. Marsily, Quantitative Hydrogeology—Groundwater Hydrology for Engineers, Academic Press, San Diego, 1986.

[7] F. Dullien, Porous Media—Fluid Transport and Pore Structure, Academic Press, San Diego, 1992.

[8] R. Helmig, Multiphase Flow and Transport Processes in the Subsurface, Springer, Berlin, 1997.

[9] R. Hilfer, Macroscopic equations of motion for two phase flow in porous media, Phys. Rev. E 58 (1998) 2090.

[10] R. Hilfer, H. Besserer, Old problems and new solutions for multiphase flow in porous media, in: A. Dmitrievsky, M. Panfilov (Eds.), Porous Media: Physics, Models, Simulation, World Scientific, Singapore, 2000, p. 133.

[11] R. Hilfer, H. Besserer, Macroscopic two phase flow in porous media, Physica B 279 (2000) 125.

[12] F. Preisach, Über die magnetische Nachwirkung, Z. Physik 94 (1935) 277.

[13] L. Neel, Theorie des lois d'aimanation de Lord Rayleigh, Cah. de Phys. 12 (1942) 1.

[14] D. Everett, W. Whitton, A general approach to hysteresis, Trans. Faraday Soc. 48 (1952) 749.

[15] A. Enderby, The domain model of hysteresis, Trans. Faraday Soc. 51 (1955) 835.

[16] A. Poulovassilis, Hysteresis of pore water. An application of the concept of independent domains, Soil Sci. 93 (1962) 405.

[17] G. Topp, E. Miller, Hysteretic moisture characteristics and hydraulic conductivities for glass bead media, Soil Sci. Soc. Am. Proc. 30 (1966) 156.

[18] A. Poulovassilis, E. Childs, The hysteresis of pore water: the non-independence of domains, Soil Sci. 112 (1971) 301.

[19] J. Philip, Similarity hypothesis for capillary hysteresis in porous materials, J. Geophys. Res. 69 (1966) 1553.

[20] Y. Mualem, Modified approach to capillary hysteresis based on a similarity hypothesis, Water Resour. Res. 9 (1973) 1324.

[21] Y. Mualem, A conceptual model for hysteresis, Water Resour. Res. 10 (1974) 514.

[22] J. Parker, R. Lenhard, A model for hysteresic constitutive relations governing multiphase flow. 1. Saturation–pressure relations, Water Resour. Res. 23 (1987) 2187.

[23] C. Land, Calculation of imbibition relative permeability for two- and three-phase flow from rock properties, Trans. AIME 243 (1968) 149.

[24] S. Hassanizadeh, M. Celia, H. Dahle, Dynamic effect in the capillary pressure–saturation relationship and its impacts on unsaturated flow, Vadose Zone J. 1 (2002) 38.

[25] C. Marle, On macroscopic equations governing multiphase flow with diffusion and chemical reactions in porous media, Int. J. Eng. Sci. 20 (1982) 643.

[26] D. Pavone, Macroscopic equations derived from space averaging for immiscible two-phase flow in porous media, Rev. Inst. Francais Petrole 44 (1989) 29.

[27] W.G. Gray, S. Hassanizadeh, Unsaturated flow theory including interfacial phenomena, Water Resour. Res. 27 (1991) 1855.

[28] I. Fatt, The network model of porous media I. Capillary pressure characteristics, AIME Pet. Trans. 207 (1956) 144.

[29] S. Bakke, P. Øren, 3-d pore-scale modeling of sandstones and flow simulations in pore networks, SPE J. 2 (1997) 136.

[30] R. Wyckoff, H. Botset, Flow of gas–liquid mixtures through unconsolidated sands, Physics 7 (1936) 325.

[31] M. Muskat, M. Meres, Flow of heterogeneous fluids through porous media, Physics 7 (1936) 346.

[32] R. Hilfer, Capillary pressure, hysteresis and residual saturation in porous media, Physica A 359 (2006) 119.

[33] R. Hilfer, Local porosity theory for flow in porous media, Phys. Rev. B 45 (1992) 7115.

[34] R. Hilfer, Geometric and dielectric characterization of porous media, Phys. Rev. B 44 (1991) 60.

[35] R. Hilfer, Transport and relaxation phenomena in porous media, Adv. Chem. Phys. XCII (1996) 299.

[36] R. Hilfer, J. Widjajakusuma, B. Biswal, Macroscopic dielectric constant for microstructures of sedimentary rocks, Granular Matter 2 (1999) 137.

[37] B. Biswal, C. Manwart, R. Hilfer, S. Bakke, P. Øren, Quantitative analysis of experimental and synthetic microstructures for sedimentary rock, Physica A 273 (1999) 452.

[38] R. Hilfer, Local porosity theory and stochastic reconstruction for porous media, in: D. Stoyan, K. Mecke (Eds.), Räumliche Statistik und Statistische Physik, Lecture Notes in Physics, vol. 254, Springer, Berlin, 2000, p. 203.

[39] R. Hilfer, Review on scale dependent characterization of the microstructure of porous media, Transp. Porous Media 46 (2002) 373.

[40] R. Hilfer, J. Widjajakusuma, B. Biswal, Quantitative comparison of meanfield mixing laws for conductivity and dielectric constant of porous media, Physica A 318 (2003) 319.

[41] R. Hilfer, R. Helmig, Dimensional analysis and upscaling of two-phase flow in porous media with piecewise constant heterogeneities, Adv. Water Res. 27 (2004) 1033.

[42] W. Smith, P. Foote, P. Busang, Capillary rise in sands of uniform spherical grains, Physics 1 (1931) 18.

[43] H. Sheta, Simulation von Mehrphasenvorgängen in porösen Medien unter Einbeziehung von Hysterese-Effekten, Ph.D. Thesis, Institut für Wasserbau, Universität Stuttgart, 1999.